

# Crystallization Behavior of Biodegradable Poly(L-lactic acid) Filled with a Powerful Nucleating Agent: *N,N'*-Bis(benzoyl) Suberic Acid Dihydrazide

Yanhua Cai,<sup>1</sup> Shifeng Yan,<sup>1</sup> Jingbo Yin,<sup>1</sup> Yinqing Fan,<sup>1</sup> Xuesi Chen<sup>2</sup>

<sup>1</sup>Department of Polymer Materials, Shanghai University, Shanghai, China 201800

<sup>2</sup>State Key Laboratory of Polymer Physics and Chemistry, Changchun Institute of Applied Chemistry, Chinese Academy of Sciences, Changchun, China 130022

Received 11 August 2010; accepted 15 October 2010

DOI 10.1002/app.33633

Published online 3 March 2011 in Wiley Online Library (wileyonlinelibrary.com).

**ABSTRACT:** *N,N'*-Bis(benzoyl) suberic acid dihydrazide (NA) as nucleating agent for poly(L-lactic acid) (PLLA) was synthesized from benzoyl hydrazine and suberoyl chloride, which was deprived from suberic acid via acylation. PLLA/NA samples were prepared by melt blending and a hot-press forming process. The nonisothermal and isothermal crystallization, spherulite morphology, and melting behavior of PLLA/NA with different contents of NA were investigated with differential scanning calorimetry, depolarized-light intensity measurement, scanning electron microscopy, polarized optical microscopy, and wide-angle X-ray diffraction. With the incorporation of NA, the crystallization peak became sharper and shifted to a higher temperature as the degree of supercooling decreased at a cooling rate of 1°C/min from the melt. Nonisothermal crystallization indicated that the presence of NA accelerated the overall PLLA crystallization. In

isothermal crystallization from the melt, the presence of NA affected the isothermal crystalline behaviors of PLLA remarkably. The addition of NA led to a shorter crystallization time and a faster overall crystallization rate; this meant that there was a heterogeneous nucleation effect of NA on the crystallization of PLLA. With the addition of 0.8% NA, the crystallization half-time of PLLA/NA decreased from 26.5 to 1.4 min at 115°C. The Avrami theory was used to describe the kinetics of isothermal crystallization of the PLLA/NA samples. Also, with the presence of NA, the spherulite number of PLLA increased, and the spherulite size decreased significantly. © 2011 Wiley Periodicals, Inc. *J Appl Polym Sci* 121: 1408–1416, 2011

**Key words:** biopolymers; blending; crystallization; differential scanning calorimetry (DSC)

## INTRODUCTION

Poly(L-lactic acid) (PLLA), which is labeled as an environmentally friendly polymer, has attracted more and more interest because of increasing environmental concern and decreasing fossil resources in recent years.<sup>1–3</sup> Usually, PLLA is produced from renewable resources, such as corn and potatoes,<sup>4</sup> with lower energy consumption; it is a biopolymer and nontoxic to the environment.<sup>5</sup> Precisely, PLLA represents an interesting alternative route to common nondegradable polymers for short-life range applications, and with the continuous developmental research of PLLA, its applications have broadened

the field from short-term applications such as packaging materials<sup>6–8</sup> to automotive interiors<sup>9–10</sup> and surgical sutures.<sup>11,12</sup> What is more, PLLA in applications is expected to be a carbon neutral material from the viewpoint of the reduction of carbon dioxide emissions and the conservation of resources.<sup>4</sup> However, up to this point, PLLA still has some disadvantages. For instance, the slow crystallization rate, low degree of crystallinity ( $\chi_c$ ), and poor heat resistance of PLLA has restricted its practical applications. Thus, it is necessary to improve PLLA to make it fully competitive with commercial thermoplastics.

Usually, the most viable method for increasing the overall crystallization rate is blending with a nucleating agent. Talc is often chosen as the nucleating agent of PLLA. It was shown that talc nucleates the crystallization of polymers through an epitaxial mechanism.<sup>13</sup> Kolstad<sup>14</sup> studied the crystallization behavior and the morphology of poly(L-lactide-*co*-meso-lactide) and poly(L-lactide-*co*-meso-lactide)/talc composites. His work showed that a strong increase in the nucleation density with the addition of talc was found in poly(L-lactide-*co*-meso-lactide).

Correspondence to: J. Yin (jbyin@shu.edu.cn) or X. Chen (xschen@ciac.jl.cn).

Contract grant sponsor: Ministry of Science and Technology of the People's Republic of China; contract grant number: 2007BAE42B00.

Contract grant sponsor: Shanghai Leading Academic Discipline Project; contract grant number: s30107.

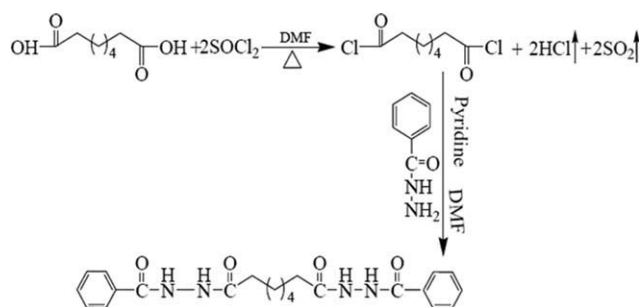


**Figure 1** Synthesis of NA (DMF = dimethylformamide).

Tianyi's<sup>15</sup> work showed that the overall crystallization rate of PLLA increased with increasing talc content. Montmorillonite is another widely used nucleating agent of PLLA.<sup>16–18</sup> Li et al.<sup>18</sup> researched the isothermal crystallization behavior of PLA/organomontmorillonite (OMMT) nanocomposites. The temperature and content of OMMT affected the induction period and half-time of overall crystallization ( $t_{1/2}$ ) for PLLA [ $100^{\circ}\text{C} \leq$  crystallization temperature ( $T_c$ )  $\leq 120^{\circ}\text{C}$ ]. Although many studies have been done to improve the crystallization of PLLA through the addition inorganic fillers, inorganic fillers are not always the most efficient compared with chemical nucleating agents.<sup>19</sup>

Recently, research efforts have shown that organic compounds can also nucleate the crystallization of PLLA.<sup>4,19–21</sup> Harris and Lee<sup>19</sup> reported that ethylene bisstearamide improved the mechanical performance of PLLA. The nucleating agent ethylene bisstearamide showed dramatic increases in the crystallization rate and final crystalline content, as indicated by isothermal and nonisothermal crystallization measurements. In isothermal crystallization from melt, with the addition of 2% ethylene bisstearamide,  $t_{1/2}$  of PLLA decreased from 38.2 to 1.8 min at  $115^{\circ}\text{C}$ . Nakajima et al.<sup>20</sup> reported that the crystallization behavior of PLLA was investigated in the presence of benzene tricarboxylamide derivatives as a nucleating agent, and benzene tricarboxylamide/cyclohexyl was the most effective nucleating agent, but it induced a complete loss of transparency of the processed material. Kawamoto and coworkers<sup>4,21</sup> reported that hydrazide compounds could serve as advanced nucleating agents for PLLA; in their studies, they obtained  $T_c$  values that were comparable to those of bulk polymers. However, they did not research the influence of hydrazide compounds on the PLLA crystallization behavior in detail.

Thus, in this study, *N,N'*-bis(benzoyl) suberic acid dihydrazide (NA) was synthesized and evaluated as a nucleating agent for PLLA. The PLLA/NA samples were prepared by melt blending and a hot-press forming process. The nonisothermal and isothermal crystallization, spherulite morphology, and melting

behavior of PLLA/NA with different contents of NA were investigated with differential scanning calorimetry (DSC), depolarized-light intensity measurement, scanning electron microscopy, polarized optical microscopy (POM), and wide-angle X-ray diffraction (WAXD).

## EXPERIMENTAL

### Materials

PLLA (2002D) was purchased from Nature Works LLC (Nebraska, United States). The other materials used in this study were analytical grade. Benzoyl hydrazine and suberic acid were procured from Beijing Chemical Reagents Co. (Beijing, China) and Chengdu Kelong Chemical Reagents Co. (Sichuan, China), respectively. *N,N*-Dimethylacetamide, thionyl dichloride, and pyridine were procured from Mianyang Rongshen Chemical Reagents Co. (Sichuan, China)

### Synthesis of NA

NA was prepared as shown in Figure 1: 0.035 mol of suberic acid and 50 mL of thionyl dichloride in the presence of *N,N*-dimethylacetamide as a catalyst were mixed, and the mixture was heated to  $80^{\circ}\text{C}$  and held at  $80^{\circ}\text{C}$  for 12 h with stirring. After the mixture was cooled to room temperature and the thionyl dichloride was evaporated *in vacuo*, the residue was suberoyl chloride.

Benzoic hydrazide and 50 mL of *N,N*-dimethylacetamide were mixed, and the mixture was purged under a nitrogen atmosphere. Suberoyl chloride was added slowly to the mixture; this was followed by the addition of pyridine, and the mixture was stirred at room temperature for 2 h, heated to  $70^{\circ}\text{C}$ , and held at  $70^{\circ}\text{C}$  for 2 h with stirring. The reaction mixture was poured into 300 mL of water and stirred; this was followed by filtration. The crude product we obtained was washed with 300 mL of water four times at room temperature and was then washed with 300 mL of methanol at  $55^{\circ}\text{C}$  to eliminate the raw materials and byproducts; the resulting product was dried *in vacuo* at  $65^{\circ}\text{C}$ .

Infrared (IR; KBr,  $\nu$ ,  $\text{cm}^{-1}$ ): 3390, 3215, 2930, 2854, 1691, 1647, 1604, 1574, 1498, 1468, 1415, 1321, 1245, 1150, 794, 692, 640. Proton nuclear magnetic resonance ( $^1\text{H-NMR}$ ; dimethyl sulfoxide, 500 MHz,  $\delta$ , ppm): 10.29 (s, 1H, NH), 9.85 (s, 1H, NH), 7.48–7.88 (m, 5H, Ar), 2.18–2.21 (t, 2H,  $\text{CH}_2$ ), 1.56–1.59 (t, 2H,  $\text{CH}_2$ ), 1.35–1.36 (d, 2H,  $\text{CH}_2$ ).

### Preparation of the PLLA/NA samples

PLLA was dried overnight at  $50^{\circ}\text{C}$  *in vacuo* to remove residual water. The blending of PLLA and

dried NA was performed in a counter-rotating mixer (Shanghai, China) with a rotation speed of 32 rpm for 5 min and then at 64 rpm for 5 min. The processing temperature was set at 185°C. The products were hot-pressed at 180°C under 20 MPa for 3 min to prepare sheets with a thickness of approximately 0.4 mm. The sheets were then cooled to room temperature by compression at room temperature under 20 MPa for 10 min. All of the samples for the crystallization studies were cut from these films.

## Characterization

### DSC

The nonisothermal crystallization behavior of PLLA was measured by a DSC Q2000 instrument (TA Instruments-Waters LLC, Pennsylvania, United States). The temperature and heat flow at different heating rate were calibrated with an indium standard. The sample was heated to 190°C and maintained at that temperature for 5 min to make sure that the polymer crystals were melted completely. Then, the samples were cooled from the melt state to 20°C at different cooling rates (1, 2, 3, and 10°C/min). Finally, the samples were reheated to 190°C at a heating rate of 10°C/min to determine the melting behavior; the melt-crystallization temperature ( $T_o$ ), melt-crystallization peak temperature ( $T_{mo}$ ), and melt-crystallization enthalpy ( $\Delta H_c$ ) were obtained from DSC. The equilibrium melting temperature ( $T_m^0$ ) was measured by the following method: the sample was heated to 190°C in a heat table and maintained at that temperature for 5 min. Then, the sample was quenched from the melt to  $T_c$  (100, 105, 110, 115, and 120°C) and held at that temperature for at least 60 min to ensure complete crystallization. At last, the sample was moved to the DSC Q2000 instrument to heat at the heating rate of 10°C/min.

### Depolarized-light intensity measurement

The overall isothermal crystallization behavior of PLLA was investigated with a GJY-III optical depolarizer (Shanghai, China) in the region from 100 to 120°C. The electronic signals transformed from the measured optical depolarizer were amplified and then recorded for further analysis.

### POM

The spherulite growth in the films was observed with an XPN-203E instrument (Changfang Optical Instrument Co., Ltd., Shanghai, China) equipped with a Canon Powershot A610 camera and a programmable temperature controller (KEL-XMT-3100A, Chaoyang Instrument Co., Ltd., Nanjing, China).

### WAXD

WAXD experiments were performed on a diffractometer (D/MAX2550, Rigaku, Tokyo, Japan) with Cu K $\alpha$  radiation (wavelength = 1.54 Å) at room temperature in the 2  $\theta$  range 5–50° at a scanning rate of 2°/min.

### Environmental scanning electron microscopy

The morphologies of the fracture surfaces of the samples were examined with a Philips XL-30 field-emission gun environmental scanning electron microscope (Eindhoven, The Netherlands) at a 15–20-kV accelerating voltage (tungsten filament). The samples were fractured and covered by gold vapors.

### IR spectra

Fourier transform infrared spectra was recorded on a Bio-Rad FTS135 spectrophotometer (Philadelphia, United States) from 4000 to 400 cm<sup>-1</sup>. The NA sample was mixed with KBr powders and pressed into a disk suitable for IR measurement.

### <sup>1</sup>H-NMR

The <sup>1</sup>H-NMR spectra were recorded on a Bruker Avance 300 spectrometer (Switzerland). The solvent was dimethyl sulfoxide.

## RESULTS AND DISCUSSION

### Nonisothermal crystallization

It was very important to investigate the nonisothermal crystallization to obtain information useful for the industrial applications of PLLA. Figure 2 shows the DSC curves of the nonisothermal crystallization from the melt at a different cooling rates. As shown in Figure 2, with different cooling rates, the crystallization peak of PLLA could almost not be detected; this showed that the crystallization of neat PLLA was very slow. With addition of NA, the crystallization peak appeared in the DSC cooling curve. Compared to the neat PLLA, the addition of NA led to a shift in the crystallization peak to a higher temperature; this indicated an increase in  $T_c$ . On the other hand, the crystallization peak for PLLA containing NA became much sharper in the cooling process; this result shows that NA served as a nucleating agent for the crystallization and increased the overall crystallization rate of PLLA.<sup>22</sup> The degree of supercooling ( $\Delta T_{mc} = T_m^0 - T_o$ ) could be expressed as the nucleating effect on crystallization. Usually, the smaller  $\Delta T_{mc}$  is, the greater nucleating effect on PLLA crystallization is. Upon cooling at 1°C/min, as shown in Table I, with increasing NA content,  $\Delta T_{mc}$  became smaller; upon the addition of 0.8% NA,

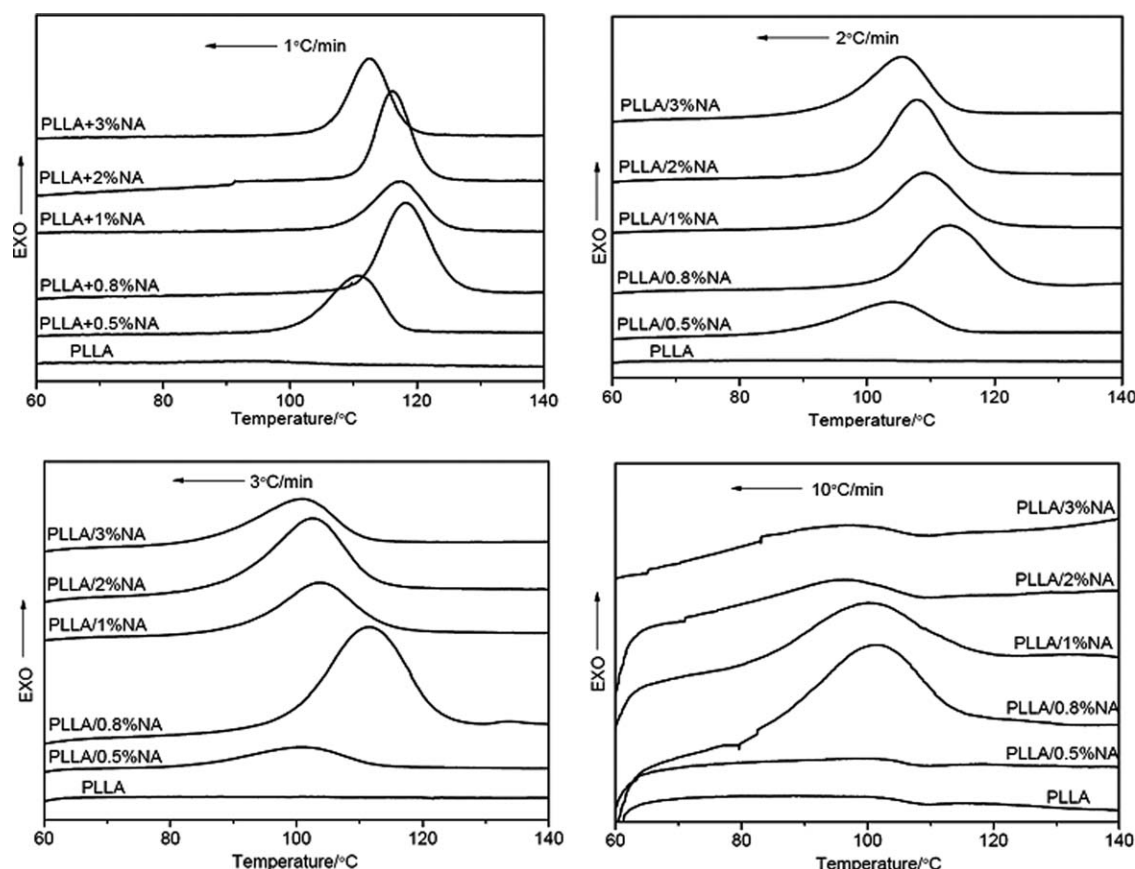


Figure 2 DSC curves for PLLA and PLLA/NA crystallized from the melt at different cooling rates.

$\Delta T_{mc}$  was smallest; this indicated that the best effect of crystallization was at 0.8% NA. Compared to the neat PLLA, with the addition of 0.8% NA,  $T_o$  increased from 105.88 to 125.57°C,  $\Delta T_{mc}$  decreased from 55.32 to 33.03°C, and  $\Delta H_c$  increased from 1.379 to 31.63 J/g.

The effects of NA on the crystallization of PLLA were investigated further by WAXD, Figure 3 shows the WAXD of the PLLA and PLLA/NA samples at a cooling rate of 1°C/min from the melt. As shown in Figure 3, the WAXD of the PLLA/NA samples was similar to that of the neat PLLA. The PLLA exhibited a very strong peak at  $2\theta = 16.6^\circ$  because of diffraction from the (110) planes and other peaks at  $2\theta = 19.2$  and  $22.3^\circ$ , occurring from the (203) and (205) planes, respectively.<sup>23</sup> With increasing NA content, the intensities of the strongest reflections (110) strengthened, and the weak peaks appeared at  $14.8^\circ$  as the (010) diffraction plane.<sup>24</sup> However, with the addition of more than 0.8% NA, the intensities of the (110) peaks became weak. This result was consistent with the aforementioned DSC results. Also, the study of the isothermal crystallization behavior proved these results, as discussed in the following text.

After nonisothermal crystallization from the melt at a cooling rate of 1°C/min, the melting behavior of

the PLLA and PLLA/NA samples were examined by DSC (a heating scan at 10°C/min). Figure 4 presents the DSC curves recorded for the heating processes for the PLLA/NA samples examined by DSC (a heating scan at 10°C/min). Apart from the neat PLLA, all of the DSC curves showed a single melting peak at a higher temperature; this was due to PLLA/NA forming perfect crystals under cooling at 1°C/min. The PLLA/NA samples melted directly without the melt recrystallization process. However, the crystallization of neat PLLA was very slow, and PLLA underwent a melt recrystallization–remelting process upon heating. The low melting peak was ascribed to the melting of primary crystals, and the high melting peak corresponded to the melting

TABLE I  
DSC Data for PLLA/NA Samples Crystallized from the Melt at a Cooling Rate of 1°C/min

Sample	$T_o$ (°C)	$T_{m0}$ (°C)	$T_m^0$ (°C)	$\Delta T_{mc}$ (°C)	$\Delta H_c$ (J/g)
PLLA	105.88	96.28	161.2	55.32	1.379
PLLA/0.5% NA	117.27	110.68	161.1	43.83	28.79
PLLA/0.8% NA	125.57	118.24	158.6	33.03	31.63
PLLA/1% NA	124.43	117.39	159.7	35.27	31.10
PLLA/2% NA	121.70	116.29	160.6	38.9	29.94
PLLA/3% NA	118.41	112.63	160.9	42.49	29.75

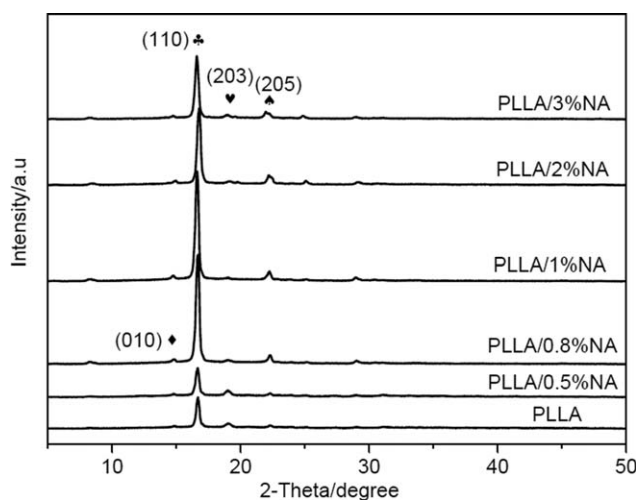


**Figure 3** WAXD patterns of the neat PLLA and PLLA/NA samples cooling from the melt at 1°C/min.

of the recrystallized crystals. The crystallization thermodynamic parameters of the neat PLLA and PLLA/NA samples are listed in Table II. By considering the melting enthalpy of 100% crystalline PLLA ( $\Delta H_m^*$ ) to be 93.7 J/g,<sup>18</sup> we estimated the value of  $\chi_c$  of PLLA in different systems. The  $\chi_c$  values of the composites were based on the following equation:

$$\chi_c = \frac{\Delta H_m}{(1 - \phi)\Delta H_m^*} \times 100\% \quad (1)$$

where  $\phi$  is the weight fraction of the filler in the composite and  $\Delta H_m$  is the heat of fusion. According to the data listed in Table II, the melting temperature ( $T_m$ ) gradually decreased, whereas  $\chi_c$  of PLLA reached a maximal value at 0.8% NA loading. This was because of the heterogeneous nucleating effect

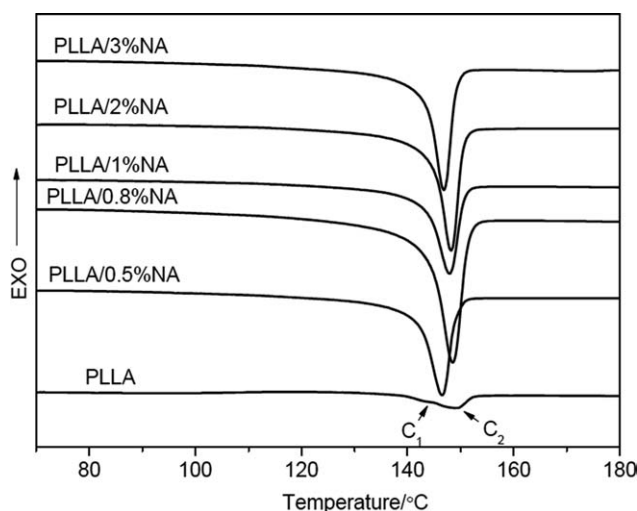


**Figure 4** DSC curves of PLLA and PLLA/NA samples with different NA contents melting at a heating rate of 10°C/min.

**TABLE II**  
Thermal Parameters of the PLLA and PLLA/NA Samples

Sample	$T_m$ (°C)	$\Delta H_m$ (J/g)	$\chi_c$ (%)
PLLA	149.37	4.381	4.68
PLLA/0.5% NA	146.31	29.49	31.6
PLLA/0.8% NA	148.15	35.04	37.7
PLLA/1% NA	147.84	33.16	35.7
PLLA/2% NA	147.95	32.36	35.2
PLLA/3% NA	146.54	30.35	33.4

of the low amount of NA, and a high amount of NA may have restricted the crystallization behavior of PLLA. Similar results were found in other systems, such as PLLA/OMMT nanocomposites.<sup>18</sup>

The dispersion of the nucleating agent in the PLLA matrix also affected the PLLA crystallization. Figure 5 shows the scanning electron microscopy images of the nucleating agent NA and the freeze-fractured surfaces of neat PLLA and PLLA/NA with various contents of NA in the same scale. As shown in Figure 5(A), the particle of the nucleating agent NA is platelike; this was favorable for improving the nucleating effect on crystallization,<sup>25</sup> and the size of the particle was only several micrometers. Neat PLLA showed a smooth, freeze-fractured surface [Fig. 5(B)]. Figure 5(C,D) shows that there existed many small NA particles, and the NA particles could disperse uniformly in the PLLA matrix with increasing NA content. Thus, the addition of NA resulted in a substantial increase in the nucleating density, and then, the crystallization of PLLA was also improved. However, with the addition of excessive NA, the nucleating agent NA tended to seriously aggregate, and it was difficult to disperse it homogeneously in the PLLA matrix [Fig. 5(E)]. This may have impeded the macromolecular segment activity and reduced the nucleating effect of the nucleating agent NA.

### Overall isothermal crystallization behavior

The isothermal crystallization behavior was investigated with the depolarized-light intensity technique<sup>26</sup> as the transmitted light intensity increased with increasing crystallinity and finally leveled off when the crystallization was complete. In our research, we used the relative light intensity ( $I_r$ ), defined by the following equation as an index of crystallinity:

$$I_r(\%) = 100 \times \frac{(I_t - I_0)}{(I_\infty - I_0)} \quad (2)$$

where  $I_t$  and  $I_0$  are the transmitted light intensity values at crystallization time of  $t$  and 0, respectively, and  $I_\infty$  is the transmitted light intensity value when the crystallization was complete. Figure 6

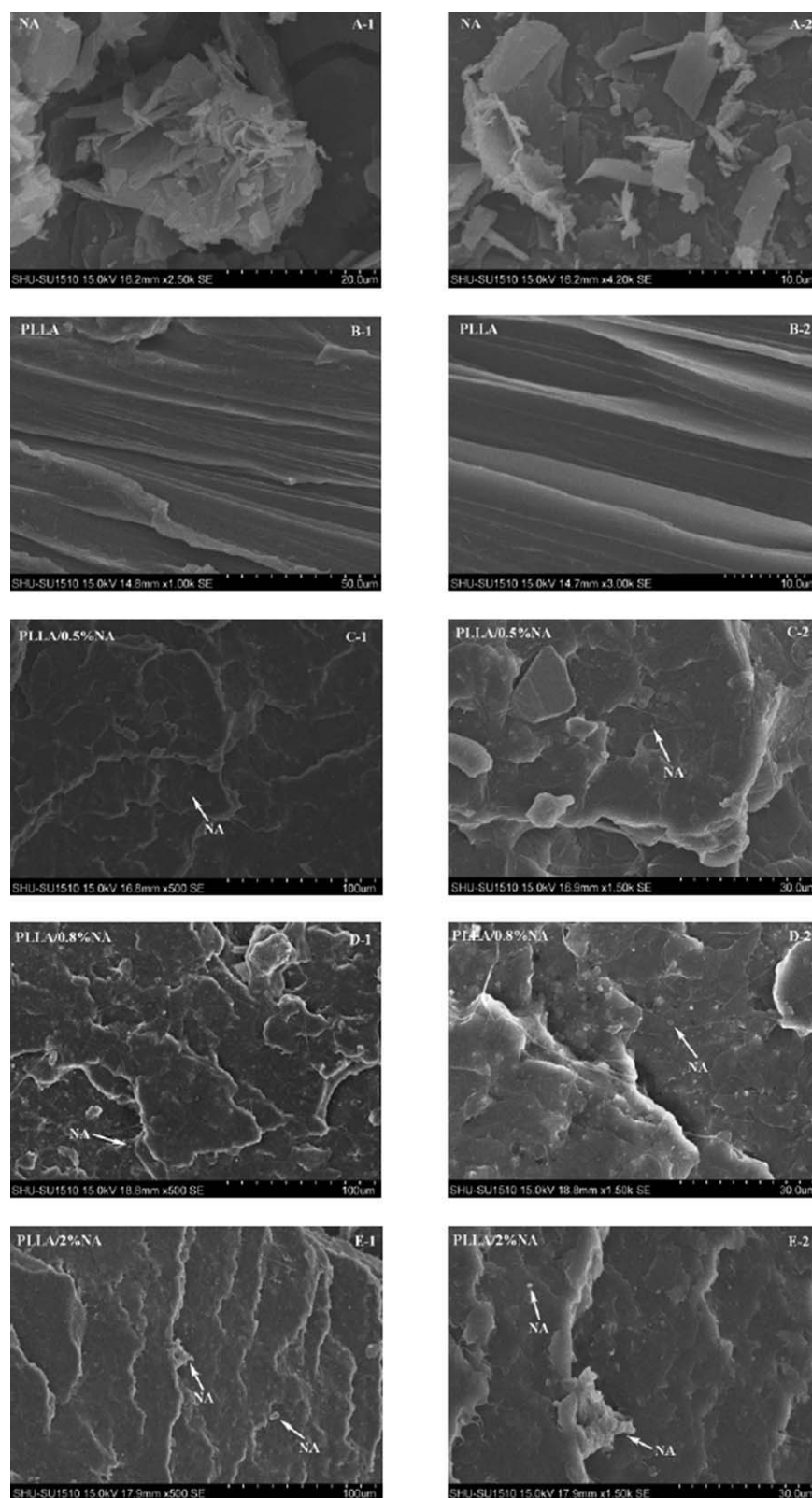


**Figure 5** Scanning electron micrographs of the nucleating agent NA, neat PLLA, and PLLA/NA samples with various contents.

shows the effects of the NA content and  $T_c$  on  $t_{1/2}$  for PLLA. First, with increasing  $T_c$ ,  $t_{1/2}$  became shorter and possessed a minimum value at 115°C;

this resulted from the enhancement of the macromolecular segment mobility with increasing  $T_c$ . However, it was hard for PLLA to form a spherulite

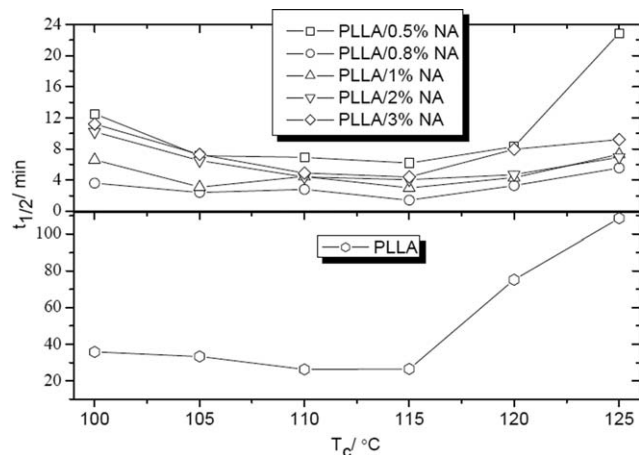


Figure 6  $t_{1/2}$  for PLLA and PLLA/NA versus  $T_c$ .

when  $T_c$  was too high because the excessive macromolecular segment activity restricted the formation of spherulites, and  $t_{1/2}$  became longer with further increases in  $T_c$ . On the other hand, the trend of  $t_{1/2}$  with NA content was similar to that of  $T_c$ . For neat PLLA,  $t_{1/2}$  decreased from 26.5 min to a minimum value of 1.4 min with 0.8% NA at 115°C. When the NA content was further increased,  $t_{1/2}$  started to become longer. Generally, the addition of more filler increased the probability of filler aggregation, which impeded the active macromolecular segment when the NA content was more than 0.8%.  $t_{1/2}$  decreased greatly with the addition of NA as it plays an excellent heterogeneous nucleation role.

The polymer isothermal crystallization process can be described by the following Avrami equation:<sup>27</sup>

$$1 - \frac{X_c}{100} = \exp(-kt^n) \quad (3)$$

where  $k$  is the crystallization rate constant ( $\text{min}^{-1}$ ) and  $n$  is the Avrami exponent.  $X_c(t)$  represents the percentage of relative crystallization after time  $t$ . Equation (3) can be transformed to eq. (4):

$$\lg \left[ -\ln \left( 1 - \frac{X_c(t)}{100} \right) \right] = \lg k + n \lg t \quad (4)$$

In this study, we used  $I_r$  as  $X_c$  in eq. (4). The obtained kinetic parameters ( $n$ ) and the  $k$  values of the neat PLLA and PLLA/NA samples are listed in Table III. It is generally agreed that  $n$  depends on the nucleation and growth mechanisms of the spherulites. For spherulite three-dimensional growth,  $n$  is 4 in a homogeneous nucleation system and 3 in a heterogeneous nucleation system.  $n$  should be an integer but is always a decimal fraction.<sup>28</sup> This might be due to the presence of crystalline branching and/or two-stage crystal growth during the crystalliza-

tion process and/or a mixed growth and nucleation mechanism.<sup>29</sup> As shown in Table III, most  $n$  values were nonintegral values between 2.5 and 5.5. That the  $n$  values of pure PLLA are around 4 in Table II shows that pure PLLA followed a homogeneous nucleation mechanism. For the PLLA/NA sample, the  $n$  values ranged between 2.5 and 5.5 with increasing  $T_c$ ; this shows that the PLLA/NA composite not only followed a heterogeneous nucleation process followed by three-dimensional crystal growth but also had another complicated nucleation mechanism.<sup>18</sup> The  $k$  values showed a similar trend with the  $t_{1/2}$  values, and the largest values occurred for PLLA/0.8% NA.

Figure 7 shows the WAXD of the PLLA/0.8% NA sample annealed at different  $T_c$  values for 0.5 h. For the PLLA/0.8% NA sample, with increasing  $T_c$ , the diffraction peaks from the (010), (110), (203), and (205) planes strengthened, and the peak at 115°C appeared to be the maximum value. These indicated

TABLE III  
Isothermal Crystallization Parameters of PLLA and PLLA/NA

Sample	$T_c$ (°C)	$n$	$k$
PLLA	100	3.5	$2.19 \times 10^{-6}$
	105	3.6	$1.88 \times 10^{-6}$
	110	4.1	$1.17 \times 10^{-6}$
	115	3.5	$7.10 \times 10^{-6}$
	120	4.3	$5.02 \times 10^{-9}$
	125	3.5	$3.46 \times 10^{-8}$
PLLA/0.5% NA	100	4.5	$8.09 \times 10^{-6}$
	105	5.6	$1.14 \times 10^{-5}$
	110	4.7	$7.75 \times 10^{-5}$
	115	2.9	$3.18 \times 10^{-3}$
	120	2.9	$1.44 \times 10^{-3}$
	125	4.4	$7.25 \times 10^{-7}$
PLLA/0.8% NA	100	3.8	$5.69 \times 10^{-3}$
	105	4.3	$1.56 \times 10^{-2}$
	110	4.6	$5.54 \times 10^{-3}$
	115	4.5	$1.19 \times 10^{-1}$
	120	4.4	$3.39 \times 10^{-3}$
	125	4.5	$2.84 \times 10^{-4}$
PLLA/1% NA	100	3.4	$1.19 \times 10^{-3}$
	105	5.1	$2.04 \times 10^{-3}$
	110	4.9	$4.89 \times 10^{-4}$
	115	5.3	$1.95 \times 10^{-3}$
	120	5.3	$2.64 \times 10^{-4}$
	125	5.2	$1.64 \times 10^{-5}$
PLLA/2% NA	100	4.5	$1.52 \times 10^{-5}$
	105	5.1	$4.16 \times 10^{-5}$
	110	3.4	$4.00 \times 10^{-3}$
	115	3.3	$7.35 \times 10^{-3}$
	120	2.7	$9.83 \times 10^{-3}$
	125	3.1	$1.57 \times 10^{-3}$
PLLA/3% NA	100	2.7	$9.56 \times 10^{-4}$
	105	2.9	$1.98 \times 10^{-3}$
	110	4.2	$8.43 \times 10^{-4}$
	115	3.9	$1.91 \times 10^{-3}$
	120	4.1	$1.39 \times 10^{-4}$
	125	5.6	$2.18 \times 10^{-6}$

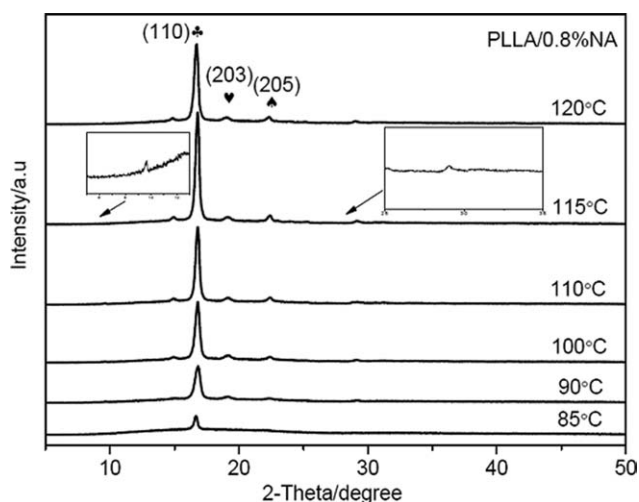


**Figure 7** WAXD patterns of the PLLA/NA samples annealed for 0.5 h at different  $T_c$  values.

that the crystallization of the PLLA/NA samples at 115°C was easier than those at other  $T_c$  values, which was the same result as for the aforementioned crystallization rate. At the same time, two weak peaks appeared at 9.6 and 28.9°.

The spherulite morphology of NA-containing PLLA was compared with that of the neat PLLA by POM. Figure 8 shows the POM image of the PLLA and PLLA/0.8% NA samples during the isothermal crystallization process at 115°C. PLLA had a typical spherulite structure, which is shown clearly in the POM images in Figure 8. The spherulites of the neat PLLA were spherical in shape during the initial stages of crystallization [Fig. 8(A)], but the spherulite density was small; this was consistent with the results reported by Pan et al.<sup>30</sup> However, PLLA/0.8% NA displayed the higher nuclea-

tion speed among the two samples [Fig. 8(D)]. This further indicated that the NA particles acted as an effective heterogeneous nucleation agent. During the latter stages of crystallization, the spherulite number of the PLLA/0.8% NA samples further increased, and the spherulites impinged on their neighbors [Fig. 8(E)]. Finally, the spherulites formed structures that pervaded the entire mass of the material, and the boundaries were indistinct [Fig. 8(C,F)], and the spherulite size of the neat PLLA was larger than that of the PLLA/0.8% NA sample. As shown in the figures, the total crystallization rate of PLLA/0.8% NA was much higher than that of neat PLLA.

Until now, there existed two nucleating mechanisms to explain the accelerated nucleation of nucleating-agent-containing polymers, namely, the mechanisms of chemical and epitaxial nucleation. In chemical nucleation, a chemical interaction between the polymer and nucleating agent occurs; this results in changed structures of the polymer matrix and nucleating agent, and this can induce the nucleation of the polymer chains.<sup>31</sup> A chemical interaction might have been expected to occur between PLLA and the nucleating agent NA, and we presumed that hydrogen bonding between C=O in the PLLA molecule and N—H of the nucleating agent NA came into being according to their functional groups analysis. This hydrogen-bonding interaction mechanism was also used to explain the interaction between PLLA and other fillers;<sup>32</sup> further studies are in progress to explore the possible mechanism.

## CONCLUSIONS

The nonisothermal and isothermal crystallization, spherulite morphology, and melting behavior of

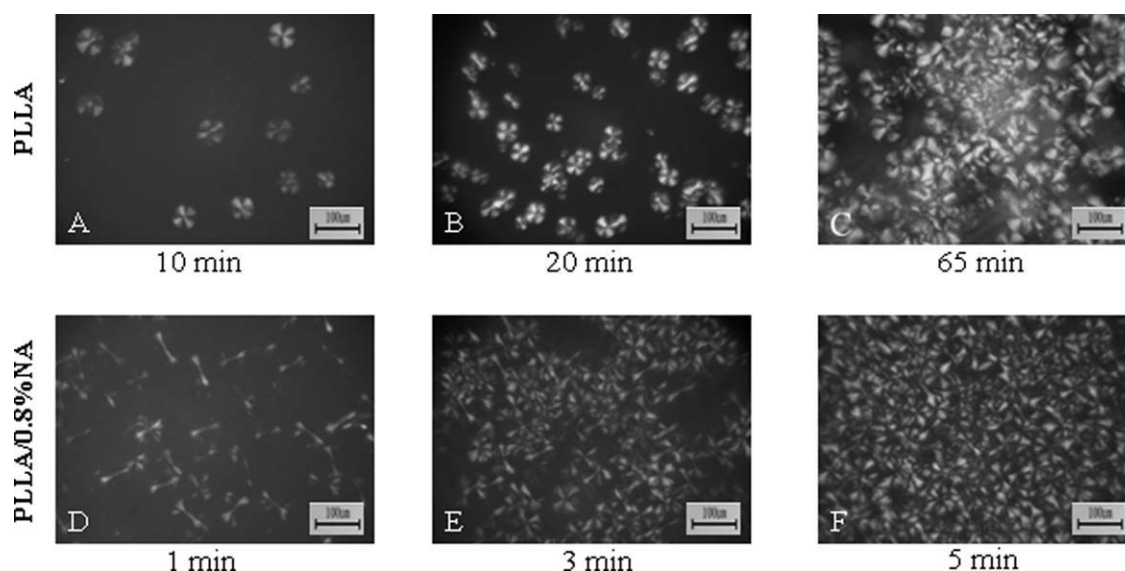


**Figure 8** POM images of the PLLA and PLLA/0.8% NA samples during isothermal crystallization at 115°C.



PLLA/NA with different contents of NA were investigated. These results show that NA, as a kind of heterogeneous nucleation agent, significantly improved the crystallization of PLLA. The use of NA led to the shift of the melt crystallization to a higher temperature, and crystallization peak became much sharper in the melting crystallization process. Upon cooling at 1°C/min, with the addition of 0.8% NA,  $T_o$  increased from 105.88 to 125.57°C,  $\Delta T_{mc}$  decreased from 55.32 to 33.03°C, and  $\Delta H_c$  increased from 1.379 to 31.63 J/g. In isothermal crystallization from melt, upon the addition of 0.8% NA,  $t_{1/2}$  of PLLA/NA decreased from 26.5 to 1.4 min at 115°C. The neat PLLA spherulites followed a three-dimensional growth though the PLLA/NA samples and not only followed a heterogeneous nucleation process followed by a three-dimensional crystal growth but also had other complicated nucleation factors. The addition of NA led to an increase in the nucleating density. The nucleating mechanism of PLLA/NA was proposed to be the hydrogen-bonding interaction between C=O in the PLLA molecule and N—H in the nucleating agent NA.

## References

1. Yu, Z. Y.; Yin, J. B.; Yan, S. F.; Chen, X. S. *Polymer* 2007, 48, 6439.
2. Lin, T. T.; Liu, X. Y.; He, C. B. *J Phys Chem B* 2010, 114, 3133.
3. Shieh, Y. T.; Liu, G. L.; Twu, Y. K.; Wang, T. L.; Yang, C. H. *J Polym Sci Part B: Polym Phys* 2010, 48, 145.
4. Kawamoto, N.; Sakai, A.; Horikoshi, T.; Urushihara, T.; Tobita, E. *J Appl Polym Sci* 2007, 103, 198.
5. Tuominen, J.; Kylmä, J.; Kapanen, A.; Venelampi, O.; Itavaara, M.; Seppälä, J. *Biomacromolecules* 2002, 3, 445.
6. Viljanmaa, M.; Södergård, A.; Törmälä, P. *Int J Adhes Adhes* 2002, 22, 219.
7. Viljanmaa, M.; Södergård, A.; Törmälä, P. *Int J Adhes Adhes* 2002, 22, 447.
8. Viljanmaa, M.; Södergård, A.; Mattila, R.; Törmälä, P. *Polym Degrad Stab* 2002, 78, 269.
9. Guo, W. J.; Bao, F. C.; Wang, Z. *China Wood Ind* 2008, 22, 12.
10. Yin, J. B.; Yu, Z. Y.; Wang, Y. J.; Lu, X. C.; Yan, S. F.; Chen, X. S. *Chin. Pat. CN101177523A* (2008).
11. Pirkka, M.; Timo, P.; Pertti, T.; Timo, W. *Biomaterials* 2002, 23, 2587.
12. Dilek, S. K.; Aysen, T.; Petek, K.; Feza, K.; Vasif, H. *Biomaterials* 2005, 26, 4023.
13. Haubruge, H. G.; Daussin, R.; Jonas, A. M.; Legras, R. *Macromolecules* 2002, 36, 4452.
14. Kolstad, J. J. *J Appl Polym Sci* 1996, 62, 1079.
15. Ke, T. Y.; Sun, X. Z. *J Appl Polym Sci* 2003, 89, 1203.
16. Jong, H. L.; Tae, G. P.; Ho, S. P.; Doo, S. L. *Biomaterials* 2003, 24, 2773.
17. Lim, L.-T.; Auras, R.; Rubino, M. *Prog Polym Sci* 2008, 33, 820.
18. Li, X. X.; Yin, J. B.; Yu, Z. Y.; Yan, S. F.; Lu, X. C.; Wang, Y. J.; Cao, B.; Chen, X. S. *Polym Compos* 2009, 30, 1338.
19. Harris, A.-M.; Lee, E. C. *J Appl Polym Sci* 2008, 107, 2246.
20. Hajime, N.; Masahiko, T.; Yoshiharu, K. *Macromol Mater Eng* 2010, 295, 460.
21. Naoshi, K.; Atsushi, S.; Takahiro, H.; Tsuyoshi, U.; Etsuo, T. *J Appl Polym Sci* 2007, 103, 244.
22. Yan, S. F.; Yin, J. B.; Yang, Y.; Dai, Z. Z.; Ma, J.; Chen, X. S. *Polymer* 2007, 48, 1688.
23. Santis, P. D.; Kovacs, A. J. *Biopolymers* 1968, 6, 299.
24. Hergeth, W. D.; Lebek, W.; Stettin, E.; Witkowski, K.; Schmutzler, K. *Makromol Chem* 1992, 193, 1607.
25. Yan, B. *Poly(lactic Acid)*; Chemical Industry Press: Beijing, 2007; Chapter 3, p 76.
26. Miyata, T.; Masuko, T. *Polymer* 1998, 39, 5515.
27. Avrami, M. *J Chem Phys* 1940, 8, 212.
28. Alamo, R. G.; Mandelkern, L. *Macromolecules* 1991, 24, 6480.
29. Hong, Z. K.; Zhang, P. B.; He, C. L.; Qiu, X. Y.; Liu, A.; Chen, L.; Chen, X. S.; Jing, X. B. *Biomaterials* 2005, 26, 6296.
30. Pan, P. J.; Liang, Z. C.; Cao, A.; Inoue, Y. S. *ACS Appl Mater Interfaces* 2009, 1, 402.
31. Legras, R.; Mercier, J. P.; Nield, E. *Nature* 1983, 304, 432.
32. Zhou, S. B.; Zheng, X. T.; Yu, X. J.; Wang, J. X.; Weng, J.; Li, X. H.; Feng, B.; Yin, M. *Chem Mater* 2007, 19, 247.